



# A Simple Explanation on The Nobility of Gold Comparing to Other Metals: A First-Principles Study

Eduardus O. Kristianto<sup>1</sup>, Samuel E. P. P. Masan<sup>2,3</sup>, Wahyu A. E. Prabowo<sup>2,4</sup>, Febdian Rusydi<sup>1,2\*</sup>, Muhammad Iqbal<sup>5</sup>, Irzaman<sup>6</sup>, Widagdo S. Nugroho<sup>7</sup>

<sup>1</sup>Department of Physics, Faculty of Science and Technology, Universitas Airlangga, Jl. Mulyorejo, Surabaya 60115, INDONESIA

<sup>2</sup>Research Center for Quantum Engineering Design, Faculty of Science and Technology, Universitas Airlangga, Jl. Mulyorejo, Surabaya 60115, INDONESIA

<sup>3</sup>Department of Precision Engineering, Graduate School of Engineering, Osaka University, 2-1 Yamadaoka, Suita, Osaka 565-0871, JAPAN

<sup>4</sup>Informatics Engineering Department, Faculty of Computer Science, Universitas Dian Nuswantoro, Semarang 50131, INDONESIA

<sup>5</sup>Department of Engineering Physics, Industrial Engineering Faculty, Institut Teknologi Bandung, Bandung 40132, INDONESIA

<sup>6</sup>Department of Physics, Faculty of Mathematics and Science, Institut Pertanian Bogor, Meranti Street, Dramaga, Bogor 16680, INDONESIA

<sup>7</sup>Department of Veterinary Public Health, Faculty of Veterinary Medicine, Universitas Gadjah Mada, Yogyakarta 55281, INDONESIA

\*Corresponding Author

DOI: <https://doi.org/10.30880/ijie.2022.14.02.016>

Received 13 December 2021; Accepted 18 March 2022; Available online 01 June 2022

**Abstract:** We evaluate the reactivity of the Au surface towards H<sub>2</sub> and compared the reactivity with Ag, Cu, and Pt surfaces. The reactivity is represented by the H<sub>2</sub> dissociation energy over each surface. Their dissociation energies were calculated based on DFT calculation with PBE functional and PAW pseudopotential. The calculation results show that the Pt surface is the most reactive, followed by the Cu, Ag, and Au surfaces. The PDOS illustrates the d-band center is above Fermi level only on the Pt surface which indicates that it is the most reactive towards H<sub>2</sub>. The adsorbate charge shows that Cu donates the most electrons, trailed by Ag and Au. This study concludes that Au surface is the most inert among the other three metals. This inertness is a characteristic that defines a noble metal.

**Keywords:** Density Functional Theory, noble metal, adsorption energy, molecule–surface interaction, transition metal reactivity, d-band center, electron donation

## 1. Introduction

It has been known that Au is the noblest of all metals. [1,2] To put it simply, the nobleness of Au is shown from its inertness. Au is hard to react with molecules like O<sub>2</sub> and H<sub>2</sub>O [3,4], which by and large react effectively with other transition metals. On the other hand, Au can still form stable alloys with other metals. [5] Moreover supported Au surfaces show a high catalytic activity for carbon monoxide oxidation, water gas shift, and hydrogenation reaction.

\*Corresponding author: [rusydi@fst.unair.ac.id](mailto:rusydi@fst.unair.ac.id)

[4,6-8] These makes Au reactivity intriguing to investigate. Theoretical study of the nobleness of Au has been done comprehensively by Hammer. [1] Hammer compared the nobleness of Au with other metals, namely Cu, Pt, and Ni, based on the  $H_2$  dissociation reaction on the surfaces. Hammer concluded that calculation results based on density functional theory (DFT) of activation barrier and adsorption energy are proportional to (1) number of filled antibonding states and (2) orbital overlap magnitude between surface and adsorbate. The combination of these two factors determines the strength of the adsorbate and metal interactions. In the present study, the nobleness of Au is explained in a simpler manner. We compared the reactivity of Au with other transition metals in the same group (Ag and Cu) and in a different group (Pt). The reactivity is studied from  $H_2$  dissociation energy on the surfaces, without considering the activation barrier. Even so, Grimme's semiempirical correction [9] is incorporated into the DFT calculation to take the dispersion effect between adsorbate and metal. Other than analyzing DOS (bonding and antibonding states) as Hammer did, we additionally analyzed the atomic charge density to explain the reactivity levels of these metals.

## 2. Methodology

We used Au, Ag, Cu, and Pt surfaces with Miller index (111). The lattice constants for these surfaces are  $4.07\text{\AA}$  [10],  $4.08\text{\AA}$  [11],  $3.68\text{\AA}$  [12], and  $3.94\text{\AA}$  [13] respectively. Slab model of the surfaces is constructed using 27 atoms which are divided into three layers. Optimization is done on the top layer while the latter two layers are fixed to maintain the bulk structure. Optimization calculation is done before and after the  $H_2$  dissociated above the surfaces. Before dissociation,  $H_2$  is placed  $6\text{\AA}$  on the normal direction of the surfaces. After dissociation, those H atoms are placed  $1\text{\AA}$  on top, bridge, and hollow positions of the surfaces (see Figure 1). However, H atoms (and the metal atoms of the uppermost surface layer) are free to move during optimization. This procedure is typical for DFT calculation on molecule adsorption on surface. [14-18] Dissociation reaction energy is the difference between the energy of the  $H_2$ —surface system before and after dissociation.

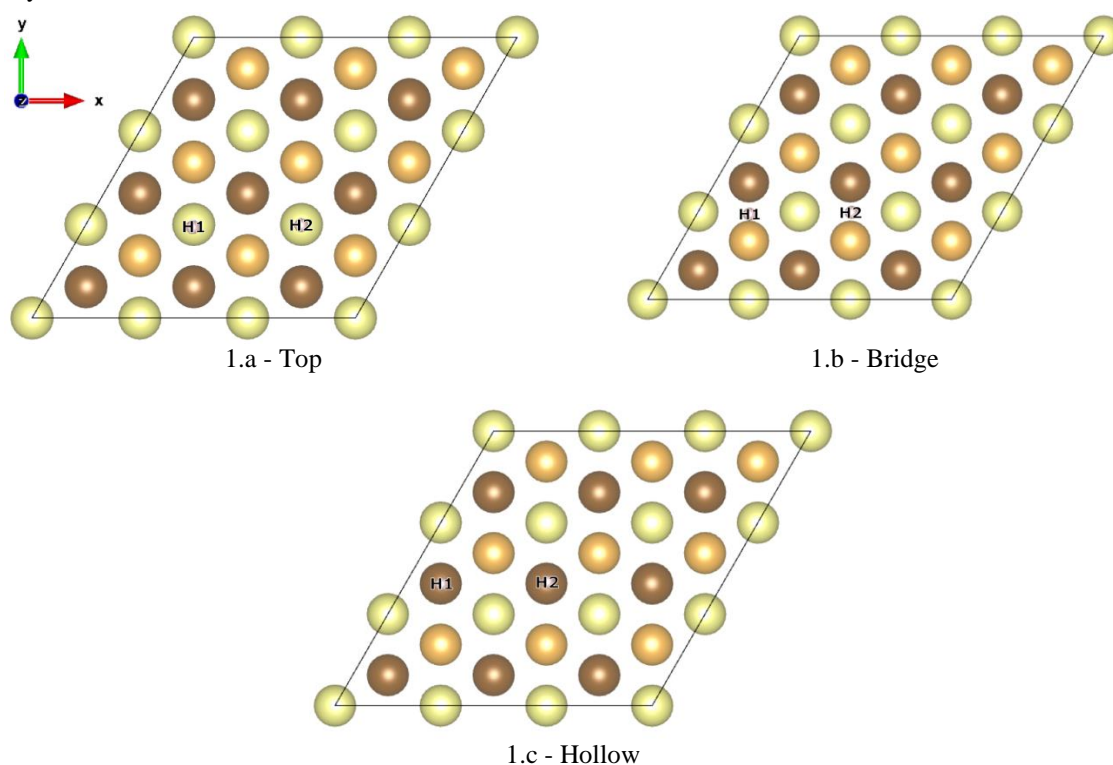


**Fig. 1 - Top view of H atoms position after being dissociated on the surfaces. Bright circles are the metal atoms of the uppermost layer, while darker circles denote metal atoms of the deeper layers**

The optimization calculation is done based on DFT using Quantum ESPRESSO software. [19,20] For that, approximation of exchange-correlation functional is done using PBE functional. [21] PAW pseudopotential is applied to model the core electron dynamics. [22] Dispersion effect are considered using Grimme's semiempirical correction. [9] We use the k-point Monkhor-Pack [23] whose grid size we obtained through convergence test along with two other parameters: the magnitude of kinetic energy cutoff for wavefunction, and the vacuum height. The results of the convergence test are presented in Table 1. For Self-Consistent Field (SCF) calculation, this study uses force threshold for geometric optimization with a magnitude of  $10^{-3}$  Ry/Bohr while the energy threshold with a magnitude of  $10^{-6}$  Ry.

In essence, DOS are also analyzed by projecting it onto atomic orbitals and calculating the atomic charge density using Bader Charge Analysis version 1.04. [24]

**Table 1 - Cut-off energy ( $E_{cut}$ ), k-point, and vacuum height (Vac.) for each surface obtained through convergence test**

Surface	$E_{cut}$ (eV)	k-point	Vac. (Å)
Au(111)	510	9	12
Ag(111)	570	8	11
Pt(111)	490	5	12
Cu(111)	510	8	11

### 3. Results and Discussion

Table 2 gives information about the adsorption configuration of  $H_2$  after dissociated on the Au (111), Ag (111), Cu (111), and Pt (111) along with their energies. For Au (111) and Pt (111), the H atoms can be adsorbed on top, bridges, and hollow. Whereas in Ag (111) and Cu (111), H atoms can only be adsorbed on bridges and hollows, with hollow being the majority of adsorption sites. The energy difference between configurations indicates that H atoms tend to be adsorbed at the hollow sites for Au (111), Ag (111), and Cu (111), and the top sites for Pt (111). Figure 2 shows the difference in dissociation energy on each surface. The most positive  $H_2$  dissociation energy is in Au (111), followed by Ag (111), Cu (111), and Pt (111).  $H_2$  dissociation above Au (111) and Ag (111) are endothermic while on Cu (111) and Pt (111) are exothermic. This means, energetically, the dissociation reaction of  $H_2$  above Au (111) and Ag (111) are harder compared to Cu (111) and Pt (111).

**Table 2 - Adsorption configuration of dissociated  $H_2$  (H1, H2), their separation distance ( $d$ ) in Å, and the energy of  $H_2$ -surface system ( $E$ ) in eV. The adsorption sites of those H atoms on top, bridge, and hollow are represented by T, B, and H. The energy is relative to the site with the most negative energy value**

No.	Au (111)			Ag (111)			Cu (111)			Pt (111)		
	H1,H2	$d$	$E$	H1,H2	$d$	$E$	H1,H2	$d$	$E$	H1,H2	$d$	$E$
1.	T, T	3.36	0.42	H,B	3.08	0.00	H,B	2.67	0.00	T,T	2.88	0.00
2.	B, B	3.33	0.05	H,H	3.07	0.01	H,H	2.66	0.00	B,B	2.84	0.22
3.	H, H	3.36	0.00							H,H	2.87	0.27

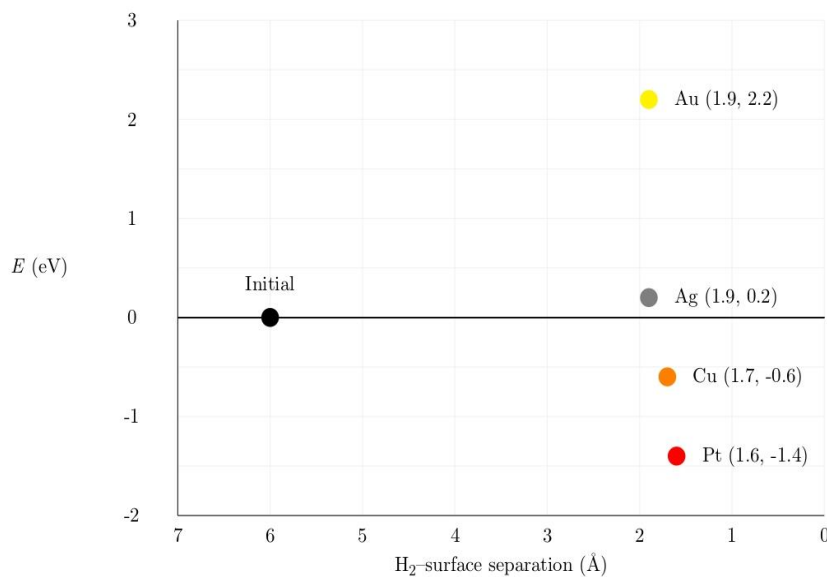


**Fig. 2 -  $H_2$ -surface energy. The energy is relative to the initial state, when  $H_2$  is located 6Å from the surface. In the final state, the  $H_2$  is dissociated**

Figure 3 shows the orbital interaction between Au (111) surface and the adsorbed H<sub>2</sub> atoms. Similar interactions also happen for Ag (111), Cu (111), and Pt(111) surfaces. This shows that H undergoes chemisorption on these surfaces. Figure 4 shows the DOS from the H<sub>2</sub>-surface system which are projected against the 1s H and d-band surfaces. The PDOS for 1s H orbital shows bonding and antibonding states from the interaction with the d-band surface. The bonding state is found to be the most dominant and formed below the energy value of -5 eV. The antibonding state is formed around the Fermi level. For Au (111), Ag (111), and Cu (111), the antibonding state is on the left side of the Fermi level, while for Pt (111), it is the other way around. The filling of the antibonding state for Au (111), Ag (111), and Cu (111) by electrons produces a repulsive force between H and these surfaces which results in their higher energy compared to Pt (111).

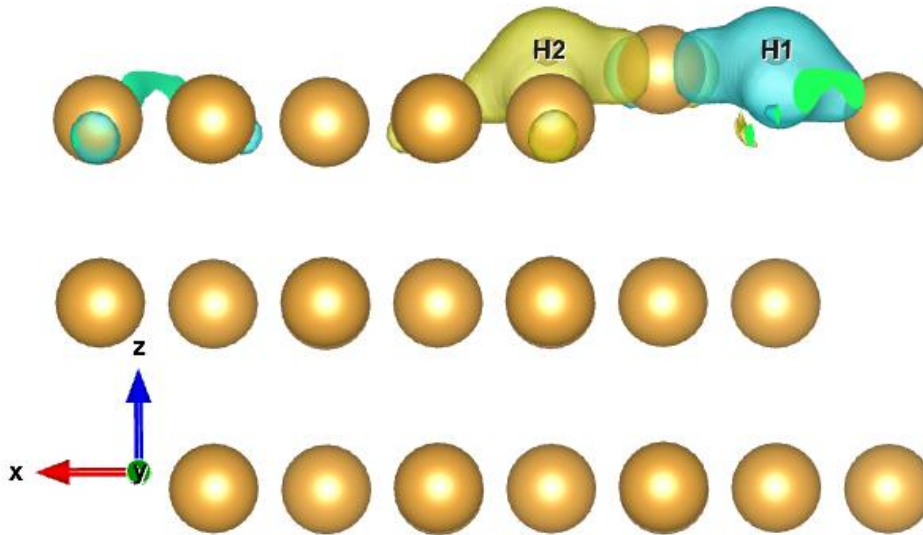


**Fig. 3 - Isosurface molecular orbital of H<sub>2</sub>-Au on an energy level of -7.78 eV (relative to Fermi energy) and isovalue 0.05. Each blue and yellow color shows positive and negative phases respectively**

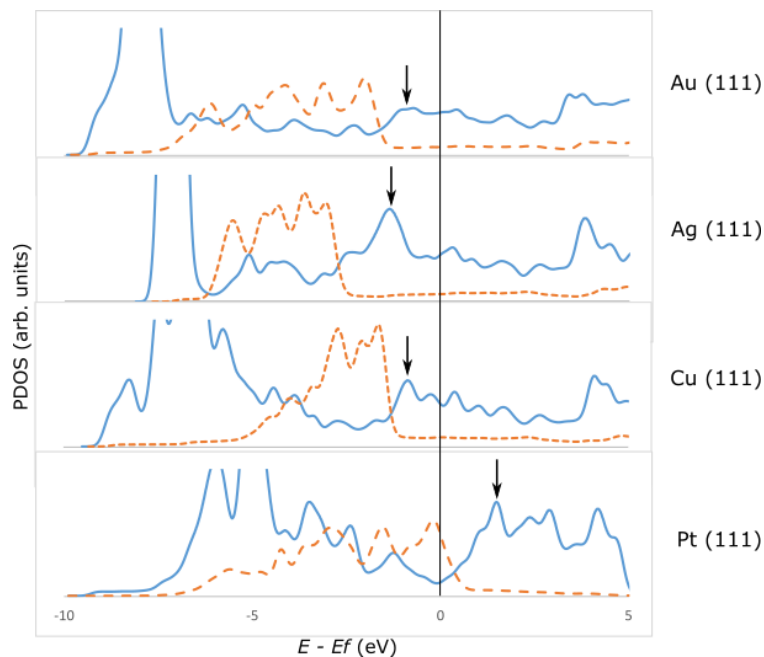


**Fig. 4 - Solid line: Density of States (DOS) of H<sub>2</sub>-surface projected onto the 1s H orbital. Dashed line: DOS clean surface projected onto d-bands. The arrows indicate the antibonding states between 1s H and d-bands surface. The energy is relative to Fermi energy**

The position of the antibonding state is in line with the position of d-band surface. The d-bands of Au(111), Ag(111), and Cu(111) are totally located on the left side of the Fermi level, while a part of Pt(111) d-band is located on

the right side of the Fermi level. As a result, it can be known from the d-band position that Pt (111) is more reactive compared to Cu (111), Ag (111), and Au (111). On the periodic table of elements, Au, Ag, and Cu are in Group 1B while Pt is in Group 8B. Hence, the reactivity of metals in various groups can be explained based on their d-band position towards Fermi level. Table 3 shows the charge of the adsorbed H atoms. Au (111), Ag (111), Cu (111), and Pt (111) altogether donate their electrons to the H atoms, causing the H atoms to have a negative charge. Even so, it can be known from the charge that Cu (111) donates the most electrons, followed by Ag (111), Au (111), then Pt (111). The order of the ability to donate electrons by Cu, Ag, and Au are in the same trend with H<sub>2</sub> dissociation energy for those metals (Figure 1). The three metals are in the same group on the periodic table of elements. Henceforth, the reactivity of metals on a particular group can be explained based on the ability to donate electrons to the adsorbate.

**Table 3 - Charges of the adsorbed hydrogens**

No.	Surface	H1	H2
1.	Au(111)	-0.082	-0.062
2.	Ag(111)	-0.208	-0.205
3.	Pt(111)	-0.302	-0.307
4.	Cu(111)	-0.041	-0.040

#### 4. Conclusion

We have successfully evaluated the reactivity of Au, Ag, Cu, and Pt metals based on the H<sub>2</sub> dissociation energy on those metals. The order from least reactive to most reactive is Au, Ag, Cu, and Pt. We have explained the reactivity order of these metals based on (1) the d-band position of the metal to Fermi level and (2) its ability to donate electrons to the adsorbate. The d-band of (Pt) is partially filled with a higher reactivity compared to metals in Group 1B (Au, Ag, and Cu) whose d-bands are fully filled. Within the same group, the ability of a metal to donate its electron to adsorbate is proportional to its reactivity. Cu donates the most electrons to H<sub>2</sub>, followed by Ag, then Au. These results corroborate the reactivity order of those three metals in Group 1B.

#### Author Contribution

Conceptualization, methodology: Febdian Rusydi. Investigation: Eduardus O. Kristianto. Formal Analysis: Eduardus O. Kristianto and Samuel E. P. P. Masan. Project administration: Wahyu A. E. Prabowo. Supervision: Febdian Rusydi, Muhammad Iqbal, Irzaman, Widagdo S. Nugroho. Writing--original draft: Eduardus O. Kristianto. Writing--review & editing: Febdian Rusydi, Wahyu A. E. Prabowo, Samuel E. P. P. Masan.

#### Acknowledgement

This research is funded by *Program Riset Kolaborasi Indonesia - World Class University* number 162/UN3.15/PT/2021. All Quantum ESPRESSO calculations are performed on "Riven", the computational facility at the Research Center for Quantum Engineering Design, Universitas Airlangga.

#### References

- [1] Hammer, B., & Norskov, J. K. (1995). Why gold is the noblest of all the metals. *Nature*, 376, 653
- [2] Johnson P. B. & Christy R. W. (1972). Optical Constants of the Noble Metals. *Phys. Rev. B* 6, 4370
- [3] Canning, N.D.S., Outka, D., & Madix, R.J. (1984). The adsorption of oxygen on gold. *SurfaceScience*: 141.1, 240–254. issn: 0039-6028.
- [4] Rodriguez, José A., Senanayake, Sanjaya D., Stacchiola, Dario, Liu, Ping, & Hrbek, Jan. (2014). The Activation of Gold and the Water–Gas Shift Reaction: Insights from Studies with Model Catalysts. *Accounts of Chemical Research*, 47.3, 24191672, 773–782.
- [5] Kunter, R., & Mridha, S. (2016). Gold: Alloying, Properties, and Applications. *Reference Module in Materials Science and Materials Engineering*: Elsevier.
- [6] Haruta, M. (2011). Role of perimeter interfaces in catalysis by gold nanoparticles. *Faraday Discuss.* 152, 11-32
- [7] Hashmi, A.S.K. and Hutchings, G.J. (2006), *Gold Catalysis*. *Angewandte Chemie International Edition*, 45: 7896-7936
- [8] Zhang, Y., Cui, X., Shi, F., Deng, Y., (2012). Nano-gold Catalysis in Fine Chemical Synthesis. *Chem. Rev.* 112, 4, 2467-2505
- [9] Grimme, Stefan. (2006). Semiempirical GGA-type density functional constructed with a long range dispersion correction. *Journal of Computational Chemistry*, 27.15, 1787–1799.
- [10] Spreadborough, J. (2017). Crystallography Open Database: Information card for entry 1100138.
- [11] Spreadborough, J. (2017). Crystallography Open Database: Information card for entry 1100136.

- [12] Ohta, H. (2017). Crystallography Open Database: Information card for entry 9013022.
- [13] Bredig, G. (2017). Crystallography Open Database: Information card for entry 1011103.
- [14] Mortensen, J. J., Morikawa, Y., Hammer, B., Nørskov, J. K. (1997). Density Functional Calculations of N<sub>2</sub> Adsorption and Dissociation on a Ru(0001) Surface. *Journal of Catalysis* 169, 85-92
- [15] Morikawa, Y. (2001). Adsorption geometries and vibrational modes of C<sub>2</sub>H<sub>2</sub> on the Si(001) surface. *Phys. Rev. B* 63, 033405
- [16] Morikawa, Y., Ishii, H., Seki, K. (2004) Theoretical study of n-alkane adsorption on metal surfaces. *Phys. Rev. B* 69, 041403(R)
- [17] Nara, J., Higai, S., Morikawa, Y., (2004) Density functional theory investigation of benzenethiol adsorption on Au(111). *J. Chem. Phys.* 120, 6705
- [18] Quan, J., Muttaqien, F., Kondo, T. et al. (2019) Vibration-driven reaction of CO<sub>2</sub> on Cu surfaces via Eley–Rideal-type mechanism. *Nat. Chem.* 11, 722–729
- [19] Giannozzi, Paolo. (2009). QUANTUM ESPRESSO: a modular and open-source software project for quantum simulations of materials. *Journal of Physics, Condensed Matter*, 21.39, 395502.
- [20] Giannozzi, Paolo. (2017). Advanced capabilities for materials modelling with Quantum ESPRESSO. *Journal of Physics, Condensed Matter*, 29.46, 465901.
- [21] Perdew, John P., Burke, Kieron, & Ernzerhof, Matthias. (1996). Generalized Gradient Approximation Made Simple. *Phys. Rev. Lett.*, 77, 3865–3868.
- [22] Corso, A. D. (2014) Pseudopotentials periodic table: From H to Pu. *Computational Material Science* 95, 337
- [23] Monkhorst, Hendrik J., & Pack, James D. (1976). Special points for Brillouin-zone integrations. *Phys. Rev. B*, 13, 5188–5192.
- [24] Tang, W., Sanville, E., & Henkelman, G. (2009). A grid-based Bader analysis algorithm without lattice bias. *Journal of Physics, Condensed Matter*, 21.8, 084204.